

Model Predictive Control of a Power-split Hybrid Electric Vehicle with Combined Battery and Ultracapacitor Energy Storage

H. Ali Borhan Ardalan Vahidi

Abstract—In this paper, merits of using an ultracapacitor in combination with a battery in a power-split Hybrid Electric Vehicle (HEV) is analyzed. For this, an online optimization-based model predictive controller (MPC) is designed and a closed-loop model of the system is developed. Based on the definition of C-rate parameter which indicates the discharge intensity of the battery, a number of simulations over standard driving cycles are performed. Closed-loop simulations on a detailed model of the HEV show that adding the ultracapacitor to the ESS unit can reduce intensity of battery discharge, as indicated by the C-rate, noticeably.

I. INTRODUCTION

In all different types of HEVs, the energy storage system (ESS) is one of the degrees of freedom used to assist the engine or to recover the vehicle kinetic energy in the regenerative braking mode. In general, the ESS unit in hybrid vehicles should have the ability to provide both enough energy and also energy rate (power) over different driving conditions. Table I compares energy and power characteristics of ultracapacitors versus batteries [1]. As can be seen, batteries have better energy density than ultracapacitors but their power density or their ability to release energy in a very short time is typically poor. In addition, besides the fact that cycling life of a battery is much shorter than an ultracapacitor, cycling the battery at high depth of discharge (DOD) can significantly reduce the life of the battery [2], [3]. For instance, it is shown in [2] that in a Li-Ion battery, by increasing the DOD from 30% to 80%, the battery life is reduced from 2600 cycles to 1000 cycles. On the other hand, although the energy density of ultracapacitors is less than the batteries, their power density is generally much higher than the battery. Also the effective life cycle of ultracapacitors is in the order of a million. Based on the discussed advantages and disadvantages of batteries and ultracapacitors, using a combination of them in the ESS unit of HEVs has attracted attention recently [1],[3], [4].

The purpose of this paper is to analyze potential merits of integrating an ultracapacitor in the ESS unit of a power-split HEV and to design a model predictive controller for its energy management. Inclusion of the ultracapacitor bank adds one additional degree of freedom to the power-split hybrid system. The number of states also increases by one, which is the state-of-charge of the ultracapacitor. Besides the uncertainties in future power demands, using dynamic

Ali Borhan (corresponding author) is a PhD student of mechanical engineering at Clemson University, Clemson, SC 29634 E-mail: hborhan@clemson.edu.

A. Vahidi is an Assistant Professor of Mechanical Engineering at Clemson University, Clemson, SC 29634 E-mail: avahidi@clemson.edu.

TABLE I
PERFORMANCE COMPARISON OF BATTERIES AND ULTRACAPACITORS

	NIMH Battery	Li-Ion Battery	Ultracapacitor
Energy density (Wh/kg)	40-50	50-80	1-5
Power density (W/kg)	900-1100	1000-4000	1000-30,000
Number of cycles at 80% DOD	3000	3000	> 1000,000

programming to find the optimal solution of the fuel minimization problem becomes more computationally intensive due to the added state and input. Furthermore, dynamic programming based solutions are drive cycle dependent. On the other hand, optimization methods like ECMS ([5]) may be sensitive to their tuning parameter and having one more additional tuning factor adds further to the complexity of an ECMS approach [6]. Also Rule-based strategies have been proposed in some papers that have considered integration of ultracapacitors with batteries in HEVs. In [4], a table look-up approach determines the power split between the battery and ultracapacitor. The outcomes of their simulations in a commercial software tool illustrate the capabilities of improving the battery's life due to decreasing current output of the battery. Also in [3], based on an optimal engine operating map of Toyota Prius and the demanded power of a standard drive cycle, the ESS power in different segments of a vehicle trip is derived and a Maxwell D-cell ultracapacitor module is sized to reduce discharging power rate of the battery.

In this paper, based on model predictive control (MPC) method, an online suboptimal controller over a finite time horizon is developed and the performance is analyzed on the closed-loop model of a power-split HEV. This method was applied before by the authors in [7] to manage energy in a power-split HEV without ultracapacitor and the details are not repeated here. The paper is organized as follows: In Section II, the plant model of the system is presented. Based on the derived plant model, the control oriented model is derived in Section III which is employed as the prediction model of the MPC. Then in Section IV, the optimal problem of minimizing fuel consumption and sustaining energy in the battery is presented which will be solved online by the MPC in Section V. At the end, in Section VI, simulation results of the closed-loop model over standard driving cycles are presented. It is shown that the developed MPC-based controller can properly manage the power in the system in

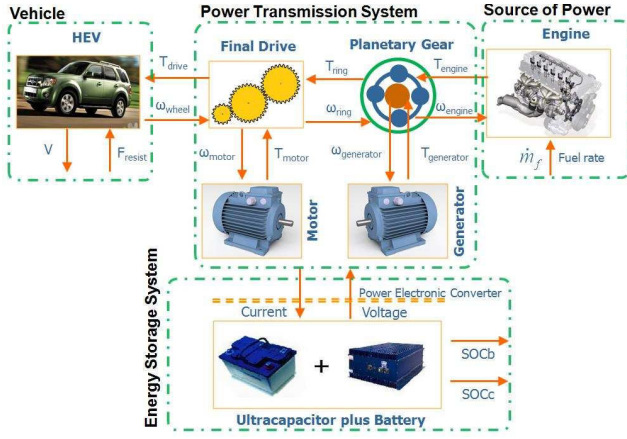


Fig. 1. A Power-Split HEV Configuration

a way that fuel consumption is minimized over a finite time horizon while the battery cycling is reduced and all varying physical constraints are satisfied.

II. THE PLANT MODEL

As it is shown in Figure 1, the model of a power-split HEV consists of a vehicle model, a power transmission model, the model of the engine as the power source and the model of the energy storage system. Each subsystem has different components with their interactions shown schematically in Figure 1. In the following subsections, the model of each subsystem is derived separately.

A. Vehicle and Power Transmission System Models

In this section, the dynamical models of the power transmission system and the vehicle are presented. More details are available in [8], [9], and [7]. As it can be observed from Figure 1, the power transmission system which is also called electric-continuously variable transmission or e-CVT, includes a planetary gear set (speed coupler) which combines the powers of the engine, motor, and generator together. This combination can be accomplished in a way that the engine operation is decoupled from the vehicle. The following assumptions are made:

- The engine, motor, and generator dynamics are modeled by first-order transfer functions.
- The inertias of pinion gears in the planetary gear set are neglected.
- The inertias of the engine, motor, and generator are lumped with the inertias of the carrier, sun, and ring gears.
- All connecting shafts in the power transmission system are rigid.
- The inertia of final transmission and the wheels are lumped with the ring gear.
- The vehicle is modeled as a lumped mass with longitudinal dynamics.

Based on these assumptions, by applying Newton's laws of motion on both the planetary gear set and the vehicle, the dynamics of the power transmission system and vehicle are derived [7],

$$\begin{aligned}
 J_{gen} \frac{d\omega_{gen}}{dt} &= T_{gen} + F \times N_S \\
 J_{eng} \frac{d\omega_{eng}}{dt} &= T_{eng} - F \times (N_S + N_R) \\
 J_{mot} \frac{d\omega_{mot}}{dt} &= T_{mot} - \frac{T_{out}}{g_f} + F \times N_R \\
 m \frac{dV}{dt} &= \frac{T_{out} + T_{brake}}{r_w} - \frac{1}{2} \rho A_f C_d V^2 - \mu mg \cos(\theta) + mg \sin(\theta)
 \end{aligned} \tag{1}$$

where J_{eng} , J_{gen} , and J_{mot} are lumped inertias of the engine, generator, and motor respectively; N_S , and N_R are the radii of the sun and ring gears; T_{eng} , T_{gen} , and T_{mot} are the engine, generator, and motor torques respectively; ω_{eng} , ω_{gen} , and ω_{mot} are the engine, generator, and motor speeds, T_{out} is the output torque of the power transmission system, T_{brake} is the friction brake torque; V , m , and A_f are the speed, mass, and frontal area of the vehicle, r_w is the wheel radius, μ is the road friction coefficient, C_D and ρ are the drag coefficient and air density respectively, g_f is the final derive ratio, θ is the road grade which is assumed to be positive when vehicle goes down a hill and g is the acceleration due to gravity. Also F is the interaction force between different parts of the gear set. There are also two kinematic equality constraints between velocities,

$$N_S \omega_{gen} + N_R \omega_{mot} = (N_S + N_R) \omega_{eng} \tag{2}$$

$$\omega_{mot} = \frac{g_f}{r_w} V \tag{3}$$

In this model, the engine, motor, generator, and brake torques are the inputs to the plant. Dynamics of the engine, motor, and generator are simplified to following first-order lags,

$$T_{eng} = \frac{1}{\tau_{eng}s + 1} \bar{T}_{eng} \tag{4}$$

$$T_{mot} = \frac{1}{\tau_{mot}s + 1} \bar{T}_{mot} \tag{5}$$

$$T_{gen} = \frac{1}{\tau_{gen}s + 1} \bar{T}_{gen} \tag{6}$$

where \bar{T}_{eng} , \bar{T}_{mot} , and \bar{T}_{gen} are the desired engine, motor, and generator and τ_{eng} , τ_{mot} , and τ_{gen} are the time constants of the engine, motor and generator, respectively.

B. The Model of the Energy Storage System (ESS)

In Figure 2, a schematic view of the energy storage system which is a combination of an ultracapacitor and a chemical battery is presented. More details on different combinations of the battery with an ultracapacitor and their power electronic topologies can be found in [2] and [10]. The following assumptions are made,

- The open circuit voltage and the internal resistance of the battery are constant.
- The dynamics of the power electronics are ignored.

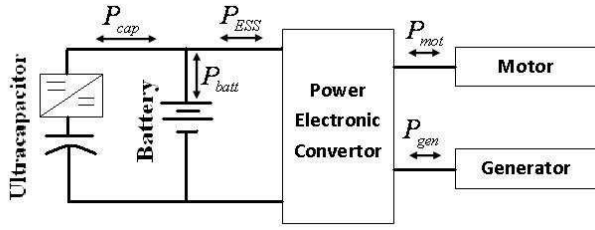


Fig. 2. Schematic view of the energy storage system (ESS).

- The power losses of the power electronic devices are modeled by a constant efficiency factor.
- The capacitance, maximum rated voltage, and the internal resistance of the ultracapacitor within the desired operating conditions are constant.
- Positive power denotes discharge and negative power denotes charge.

The state of charge is defined as the ratio between stored charge and the maximum charge capacity of a battery or an ultracapacitor. Its dynamics for the battery and ultracapacitor can be governed by the following equations [11], [7]:

$$\dot{SOC}_b = -\frac{V_{oc} - \sqrt{V_{oc}^2 - 4P_{batt}R_{batt}}}{2C_{batt}R_{batt}} \quad (7)$$

$$\dot{SOC}_c = -\frac{SOC_c V_{max} - \sqrt{(SOC_c V_{max})^2 - 4P_{cap}R_{cap}}}{2R_{cap}C_{cap}V_{max}} \quad (8)$$

where SOC_b and SOC_c are the states of the charge of the battery and ultracapacitor, V_{oc} , R_{batt} , C_{batt} , and P_{batt} are the battery's open-circuit voltage, internal resistance, capacity, and charging/discharging power, and V_{max} , R_{cap} , C_{cap} , and P_{cap} are the ultracapacitor's maximum rated voltage, internal resistance, capacitance, and power respectively. Considering the electrical power loss in the electronic power convertor unit, the ESS power and the motor and generator powers are related by,

$$P_{ESS} = \eta^{sgn(P_{mot} + P_{gen} + P_{motor}^{loss} + P_{gen}^{loss})} (P_{mot} + P_{gen} + P_{motor}^{loss} + P_{gen}^{loss}) \quad (9)$$

where η is the power convertor efficiency, $sgn(\cdot)$ the sign function, P_{mot} is motor power, P_{gen} is generator power, P_{motor}^{loss} and P_{gen}^{loss} are motor and generator power losses, and P_{ESS} is the energy storage system power. P_{ESS} is defined as:

$$P_{ESS} = P_{batt} + P_{cap} \quad (10)$$

III. CONTROL ORIENTED MODEL

In order to design a model predictive supervisory controller for online energy management of the HEV, more simplifications can be made to reduce computational effort. Before going into the details of the control-oriented model, some assumptions are made as follows,

- The lumped vehicle dynamics are pulled out of the plant model since the vehicle speed tracking is not the purpose of the controller.

- The inertial losses of the engine, motor, and generator in the power transmission system are ignored.
- To satisfy the drivability condition, the applied net torque on the wheel should be equal to the driver demanded torque,

$$T_{out} + T_{brake} = T_{driver} \quad (11)$$

- The time response of the engine, motor, and generator are negligible with respect to the ESS dynamics.
- An empirical map of the engine relates the fuel consumption rate (\dot{m}_f) to the engine speed and torque [7].
- The physical constraints of the model are summarized,

$$\begin{aligned} SOC_b^{\min} &\leq SOC_b \leq SOC_b^{\max} \\ SOC_c^{\min} &\leq SOC_c \leq SOC_c^{\max} \\ 0 &\leq \omega_{eng} \leq \omega_{eng}^{\max}, T_{eng}^{\min} \leq T_{eng} \leq T_{eng}^{\max} \\ T_{mot}^{\min} &\leq T_{mot} \leq T_{mot}^{\max}, \omega_{mot}^{\min} \leq \omega_{mot} \leq \omega_{mot}^{\max} \\ T_{gen}^{\min} &\leq T_{gen} \leq T_{gen}^{\max}, \omega_{gen}^{\min} \leq \omega_{gen} \leq \omega_{gen}^{\max} \\ P_{batt}^{\min} &\leq P_{batt} \leq P_{batt}^{\max}, P_{cap}^{\min} \leq P_{cap} \leq P_{cap}^{\max} \end{aligned}$$

where \cdot^{\min} and \cdot^{\max} denote the minimum and maximum bounds which are variable in general.

- The outputs of the model are divided into tracking and constraint outputs as,

$$y_r = \begin{bmatrix} SOC_b \\ SOC_c \\ \dot{m}_f \end{bmatrix}, \quad y_c = \begin{bmatrix} P_{batt} \\ \omega_{gen} \\ T_{mot} \\ T_{gen} \end{bmatrix}$$

- Since a goal of this work is to split the power of the ESS between the battery and the ultracapacitor optimally, a power splitting factor (denoted by r) is defined as a control input by,

$$P_{batt} = rP_{ESS} \quad (12)$$

$$P_{cap} = (1-r)P_{ESS} \quad (13)$$

where $0 \leq r \leq 1$.

Based on the above assumptions, the control oriented model can be represented by,

$$\begin{aligned} \dot{x} &= f(x, u, v) \\ y_r &= g_r(x, u, v) \\ y_c &= g_c(x, u, v) \end{aligned} \quad (14)$$

where

$$x = \begin{bmatrix} SOC_b \\ SOC_c \end{bmatrix}, \quad u = \begin{bmatrix} T_{eng} \\ \omega_{eng} \\ r \\ T_{brake} \end{bmatrix}, \quad v = \begin{bmatrix} T_{driver} \\ V \end{bmatrix}$$

x is the state vector, u the control input, and v is defined as the measured disturbances to the system which are known at each time.

IV. FUEL MINIMIZATION PROBLEM

As was mentioned above, the purpose of this paper is to design an online suboptimal controller to minimize fuel consumption such that the battery cycling is minimized and the state of charge of the battery is sustained. Since the stored energy in the ultracapacitor is small relative to the battery, there is no need to sustain ultracapacitor charge. Based on these objectives, a performance index is defined by the following 2-norm functional as,

$$J = \int_t^{t+h} \|L(x, u, v)\|^2 dt \quad (15)$$

Defining SOC_b^r and SOC_c^r as the reference values for battery and ultracapacitor states of the charge, the vector L is defined by,

$$L(x, u, v) = [w_{SOC_b}(SOC_b - SOC_b^r), w_{SOC_c}(SOC_c - SOC_c^r), w_f \dot{m}_f, w_b T_{brake}]^T \quad (16)$$

V. MPC BASED ENERGY MANAGEMENT STRATEGY

In the linear-time varying MPC framework, a predictive receding horizon controller can be designed to solve the online fuel minimization problem over a finite time horizon. An energy management strategy based on MPC method was reported before by the authors to manage energy in a power-split HEV without ultracapacitor [7]. Here, a similar approach is employed to develop an online predictive controller for a power-split HEV with the additional control input provided by the ultracapacitor. In the prediction or control-oriented model, the number of states is increased by one. The added state (SOC_c) has nonlinear dynamics and the number of degrees of freedom is increased by the power splitting factor of ESS. Different steps of the online MPC based controller, at each sample time, are summarized follows,

- Measurement or estimation of the $SOC_b(k)$ and $SOC_c(k)$ states.
- Prediction of the torque demand and vehicle speed (measured disturbances) over the prediction horizon by assuming an exponentially decaying demanded torque versus time profile with a decay rate of τ_d [7].
- Online linearization of the nonlinear prediction model around the current operating conditions.
- Application of linear MPC ([12]) online to find the control inputs or degrees of freedom.

VI. SIMULATION RESULTS AND DISCUSSIONS

In order to analyze the controller performance, two different closed-loop models of the HEV were developed. The plant model in the first one (low-order closed-loop model) is based on the control oriented model plus the lumped vehicle dynamics. The other one (high-order closed-loop model) is based on the detailed plant model derived in Section II. In both low- and high-order closed-loop models, the driver is modeled by a PI controller which tracks the vehicle speed profile. In both closed-loop models,

the same MPC is implemented. In the high-order model, a PI controller is designed to enforce tracking of the desired degrees of freedom determined by the supervisory MPC controller [7]. Also in all simulations, the sampling interval of MPC is 1 second and the prediction and control horizons are 5 steps. The prediction horizon indicates the number of prediction steps of outputs at each sample time and the control horizon indicates the number of prediction steps of control inputs to be optimized. Via various simulations, the weights are tuned by the following rules in both propelling mode (positive power demand) and braking mode (negative or zero power demand):

In the propelling mode where $T_{driver}(kT) \geq 0$:

- if $SOC_b(k) \geq SOC_b^r$
 - if $(SOC_b - SOC_b^r) \leq 0.1$
 - $w_{SOC_b} = 1, w_{SOC_c} = 0,$
 - $w_f = 100 \cdot \exp(-18 \times (SOC_b^r - SOC_b(k))), w_b = 1$
 - elseif $(SOC_b - SOC_b^r) > 0.1$
 - $w_{SOC_b} = 1, w_{SOC_c} = 0, w_f = 10, w_b = 1$
 - elseif $SOC_b(k) < SOC_b^r$
 - $w_{SOC_b} = 0, w_{SOC_c} = 0, w_f = 500, w_b = 1$
- And in the braking mode where $T_{driver}(kT) < 0$:
- $w_{SOC_b} = 1, w_{SOC_c} = 10, w_f = 5000, w_b = 0$

The desired battery state of the charge is selected at 0.7 and the desired capacitor state of the charge in the braking mode is chosen at 0.8. Also the bounds on the states of the charge are set to $0.6 \leq SOC_b \leq 0.9$ and $0.6 \leq SOC_c \leq 0.8$. In the propelling mode, the weight on the ultracapacitor state of the charge is zero and controller is allowed to use the saved energy in the ultracapacitor, as long as it is within the constraints. Also in this mode, when battery state of the charge belongs to the interval of $0.6 \leq SOC_b \leq 0.7$, the weight on the fuel consumption is defined to decrease exponentially from 100 until SOC_b becomes less than 0.6 where the fuel consumption weight is fixed at 10. Also in propelling mode, when battery's state of the charge is larger than its desired value, a large weight is put on the fuel consumption and the weight on the battery is removed to increase battery usage. In the braking mode, since the ultracapacitor can be charged faster and with higher charge density, a larger weight is defined on its state of the charge deviation from 0.8. Also, since the feasible engine speed is defined from engine idle speed to its maximum value, an engine turn on threshold equal to 1.5 kW is used in all simulations. Also in order to analyze the ESS performance with an ultracapacitor, C-rate parameter of the battery discharging is defined by,

$$C_r = \frac{P_{batt}}{0.69V_{oc}C_{batt}} \quad (17)$$

This parameter describes the discharge intensity of a battery [3],[10]. Generally, cycling the battery at high C-rates reduces the life of the battery [2]. In the next paragraphs, the average of this parameter over vehicle driving cycles is obtained to analyze the controller performance and the effect of having an ultracapacitor in the ESS. All the other

TABLE II
CHARACTERISTICS OF A PANASONIC ULTRACAPACITOR MODULE

Rated Voltage (V)	Voltage	Capacitance (F)	Resistance (mOhm)	Weight (kg)
2.5		1200	1	0.34

TABLE III
THE MPC PERFORMANCE OVER DIFFERENT DRIVING CYCLES WITH AND WITHOUT ULTRACAPACITOR

UDDS cycle			
	Equivalent Fuel Economy (mpg)		Averaged C-rate
ESS with ultracapacitor	89		0.7
ESS without ultracapacitor	79.3		2.2
Highway FET cycle			
	Equivalent Fuel Economy (mpg)		Averaged C-rate
ESS with ultracapacitor	68.1		1.3
ESS without ultracapacitor	65		3.9

parameters of the plant are extracted from the Powertrain System Analysis Toolkit (PSAT) model of Toyota Prius which has been verified in real vehicle tests by Argonne National Laboratory [13].

A. Controller Performance on the Low-order Model

To analyze the effect of using a combination of battery and ultracapacitor as the energy storage system in a power-split HEV, a closed-loop model of the vehicle with MPC as the supervisory controller was developed. In this section, the model of HEV is based on the low-order model discussed in Section III plus the lumped vehicle dynamics. Inputs to the plant in the low-order model are commanded directly by the MPC controller. Since sizing the battery and ultracapacitor is not the subject of this paper, the ultracapacitor is selected in a way that its capacity (maximum electric charge) equals one tenth of the battery capacity. Based on the specifications of the Toyota Prius's battery pack ([13]) and ultracapacitors available in the market ([1]), 100 modules of the Panasonic ultracapacitor in series are selected. The specifications of one ultracapacitor module are presented in Table II.

The simulation results of the low-order closed-loop system over two UDDS driving cycle (Urban Dynamometer Driving Schedule) and Highway FET cycle (Highway Fuel Economy Driving Schedule) are presented in Table III. On the low-order model, for both urban and highway cycles, adding the ultracapacitor without any re-sizing improves both fuel economy and the averaged battery C-rate. Also, in Figures 3 and 4, the C-rate values over UDDS cycle the cases with and without ultracapacitor are presented. As it can be observed, all C-rate's mean and standard deviation are improved when the ultracapacitor is included in the ESS unit.

B. Controller Performance on the High-order Model

In this part, in order to analyze the ultracapacitor effect on a more detailed closed-loop model of the HEV, the plant model described in Section II is used. In the high-order plant model of the HEV, the inertial dynamics of the power

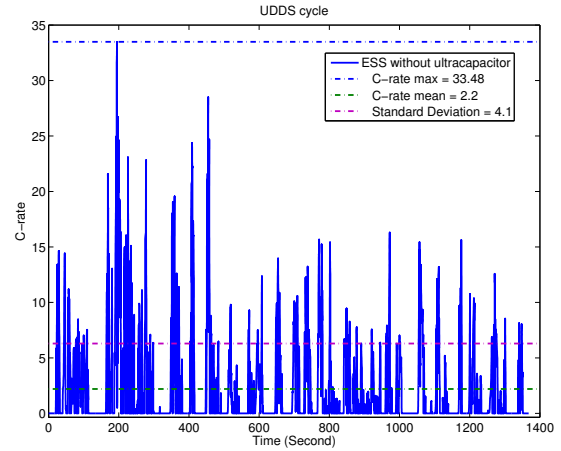


Fig. 3. C-rate results based on UDDS cycle without ultracapacitor.

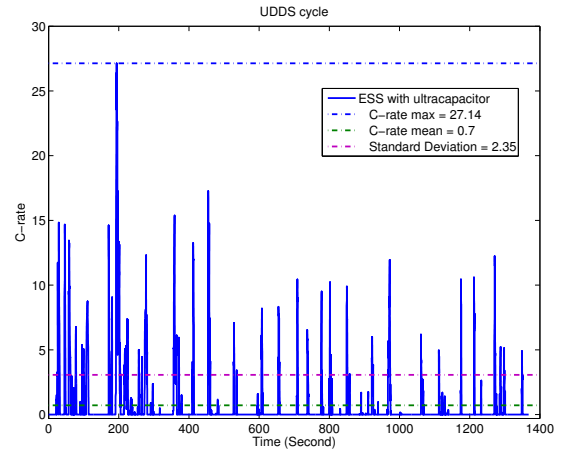


Fig. 4. C-rate results based on UDDS cycle with ultracapacitor.

transmission system and the time response of the motor, generator and engine were modeled. Since the inputs to the high-ordered model are torques plus the splitting factor, a standard PI controller was designed to control the set points evaluated by MPC. In order to compare the results with the low-ordered closed-loop model, the prediction model of the MPC and its tuning parameters were kept the same as before.

The simulation results over the UDDS and the Highway FET cycles are presented in Table IV. It can be observed that in the high-order plant model with the additional dynamics, the average C-rate of the battery is improved in particular for the UDDS cycle which has more start and stop periods. The improved C-rate is facilitated by the fact that ultracapacitors have high power densities enabling them to have a fast charge and discharge performance. But due to the additional dynamics in the plant, the fuel economy is no longer improved with the ultracapacitor. Also, in Figures 5 and 6, the C-rate values over UDDS cycle for cases with or without the ultracapacitor are presented. As it can be observed, the C-rate mean and standard deviation are improved by use of the ultracapacitor in the ESS unit.

TABLE IV
THE MPC PERFORMANCE OVER DIFFERENT DRIVING CYCLES WITH
AND WITHOUT ULTRACAPACITOR

UDDS cycle		
	Equivalent Fuel Economy (mpg)	Averaged C-rate
ESS with ultracapacitor	79.5	0.6
ESS without ultracapacitor	77.4	1.7
Highway FET cycle		
	Equivalent Fuel Economy (mpg)	Averaged C-rate
ESS with ultracapacitor	69.1	1.01
ESS without ultracapacitor	69.2	1.53

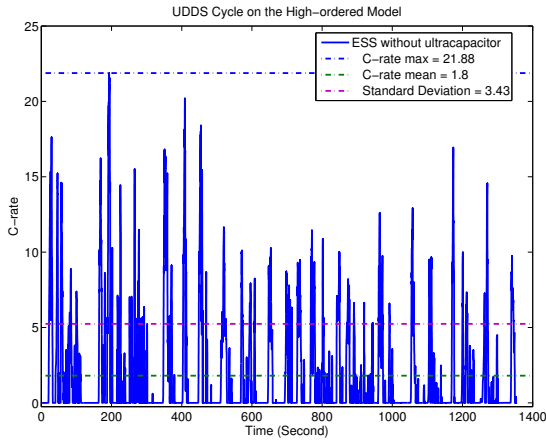


Fig. 5. C-rate results based on UDDS cycle without ultracapacitor.

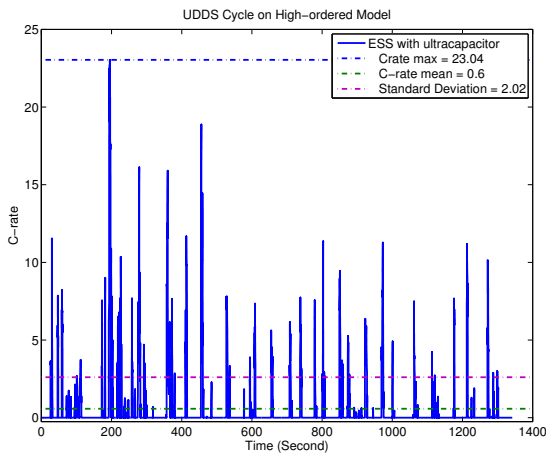


Fig. 6. C-rate results based on UDDS cycle with ultracapacitor.

VII. CONCLUSIONS

In this paper, a combination of an ultracapacitor and a battery as the energy storage unit of a power-split HEV was analyzed. First, the plant model of a power-split HEV with an ultracapacitor and battery was developed. Then, based on the control objectives to minimize both the fuel consumption and also cycling the battery at high peak powers, an online supervisory controller based on model predictive control was developed. The closed-loop simulation results show that the controller is able to manage the energy such that all

control objectives and constraints are satisfied over a finite prediction horizon. It was observed that by combining an ultracapacitor with a battery, cycling the battery at high C-rates (peak powers) is reduced significantly especially over driving cycles with more stop and start durations. The improved C-rate of the battery are expected to extend battery life and reliability.

VIII. ACKNOWLEDGEMENTS

The authors wish to thank Dr. Stefano Di Cairano, Dr. Ilya Kolmanovsky, and Dr. Anthony Phillips of Ford Motor Company for their valuable comments.

REFERENCES

- [1] A. F. Burke, "Batteries and ultracapacitors for electric, hybrid, and fuel cell vehicles," *Proceedings of the IEEE*, vol. 95, no. 4, pp. 806 – 820, 2007.
- [2] J. Miller, "Energy storage technology markets and application's: Ultracapacitors in combination with lithiumion," *The 7th International Conference on Power Electronics*, pp. 16–22, 2007.
- [3] P. McCleer J. Miller and M. Everett, "Comparative assessment of ultracapacitors and advanced battery energy storage systems in powersplit electronic-cvt vehicle powertrains," *IEEE International Conference on Electric Machines and Drives*, pp. 1513 – 1520, 2005.
- [4] A. Baisden and A. Emadi, "Advisor-based model of a battery and an ultra-capacitor energy source for hybrid electric vehicles," *IEEE Transactions on Vehicular Technology*, vol. 53, no. 1, pp. 199–205, 2004.
- [5] C. Musardo, G. Rizzoni and B. Staccia, "A-ECMS: An adaptive algorithm for hybrid electric vehicle energy management," *Proceedings of the IEEE Conference on Decision and Control*, pp. 1816– 1823, 2005.
- [6] G. Rizzoni P. Pisu, "A supervisory control strategy for series hybrid electric vehicles with two energy storage systems," *2005 IEEE Conference Vehicle Power and Propulsion*, p. pp. 8, 2005.
- [7] A. Phillips M. Kuang H. Borhan, A. Vahidi and I. Kolmanovsky, "Predictive energy management of a power-split hybrid electric vehicle," *American Control Conference*, pp. 3970 – 3976, 2009.
- [8] J. Liu and H. Peng, "Modeling and control of a power-split hybrid vehicle," *IEEE Transactions on Control Systems Technology*, vol. 16, no. 6, pp. 1242 – 1251, 2008.
- [9] F. U. Syed, M. L. Kuang, J. Czubay and H. Ying, "Derivation and experimental validation of a power-split hybrid electric vehicle model," *IEEE Transactions on Control Systems Technology*, vol. 54, no. 6, pp. 1731–1747, 2006.
- [10] O. Onar and A. Khaligh, "Dynamic modeling and control of a cascaded active battery/ultra-capacitor based vehicular power system," *IEEE Vehicle Power and Propulsion Conference*, pp. 1–4, 2008.
- [11] A. Vahidi D. Rotenberg and I. Kolmanovsky, "Ultracapacitor assisted powertrains: Modeling, control, sizing, and the impact on fuel economy," *American Control Conference*, pp. 981–987, 2008.
- [12] G. C. Goodwin, M. M. Seron and J. A. Dona, *Constrained Control and Estimation*, Springer, 2005.
- [13] Argonne National Laboratory, "Powertrain System Analysis Toolkit (PSAT) documentation," commercial software.